Available online at www.sciencedirect.com

ScienceDirect

Procedia Engineering 160 (2016) 223 – 230

Procedia Engineering

www.elsevier.com/locate/procedia

XVIII International Colloquium on Mechanical Fatigue of Metals (ICMFM XVIII)

Hydrogen transport modelling near a crack tip in a pressurized tank

A. Díaz[a]*, J.M. Alegre[a], I.I. Cuesta[a]

[a] *University of Burgos, Structural Integrity Group, Escuela Politécnica Superior, Avda. Cantabria s/n, 09006 Burgos, Spain.*
**Corresponding author, email: adportugal@ubu.es*

Abstract

With the increasing interest in the use of hydrogen as an energy carrier, a better understanding of hydrogen embrittlement affecting materials is required. In addition, hydrogen tanks suffer fatigue processes due to stress variation in filling and refuelling operations. In this context, in order to simulate hydrogen transport inside the material, a sequence of subroutines has been developed within the commercial Finite Element software ABAQUS. Diffusion equations modified by the stress state and the by existence of microstructural traps have been implemented. Models used by previous authors have been improved by implementing a stress state dependent concentration as boundary condition. Once this numerical model is established and checked, a pressurized hydrogen vessel is simulated assuming a defect in the inner wall and cyclic stresses. The influence of internal pressure, load amplitude and frequency on hydrogen concentration near the crack tip is discussed.

Peer-review under responsibility of the University of Oviedo

Keywords:

1. Introduction

Most metals and alloys suffer a toughness reduction when they are in contact with hydrogen. Thus, a change from ductile to brittle behaviour occurs. Hydrogen embrittlement requires that hydrogen enters into the metal by different surface phenomena (adsorption and absorption) and then diffuses through the bulk material.

* Corresponding author. Tel.: +0-000-000-0000 ; fax: +0-000-000-0000 .
E-mail address: adportuga@ubu.es

Peer-review under responsibility of the University of Oviedo
doi:10.1016/j.proeng.2016.08.884

Hydrogen in solid solution interacts with the crystal lattice, thereby modifying the mechanical properties of the metal or alloy. Furthermore, the interaction of hydrogen with lattice defects, such as vacancies, dislocations, grain boundaries or inclusions, also plays a crucial role. Progress must be made towards a greater understanding of these phenomena comprising various scales with the objective of predicting and preventing the failure of industrial components subjected to hydrogen embrittlement. This paper implements a diffusion model that considers defects in the metal lattice and allows to locate where the highest hydrogen concentrations are produced near a crack tip. In particular, a vessel containing pressurized hydrogen gas is modelled.

Hydrogen has emerged as an alternative for the energy industry; from H_2, a fuel cell gives energy without producing polluting waste, hence generating great expectations for sustainable mobility. Hydrogen storage optimization has revived the need to model the interaction of hydrogen with various materials and especially to solve the challenge of embrittlement. High-pressure gaseous hydrogen is the least expensive storage method with relatively technical simplicity, thus it constitutes the first approach to the large-scale management of hydrogen [1].

In this paper, a metal vessel without liner and without reinforcement or wrapping is modelled, i.e. a Type I hydrogen tank. Usually these containers are made of austenitic stainless steels or aluminium alloys, but medium and high strength steels are being proposed in order to reduce thickness and total weight. Here, the AISI 4130 steel is selected for simulations. The problem of high strength steels is that they are very susceptible to hydrogen embrittlement. In addition, the filling and fuelling operations produce cyclic loads that might cause fatigue. The initiation and subsequent fatigue propagation of cracks is influenced by the hydrogen concentration within the material. Therefore, the main objective of this paper is to find the hydrogen concentrations produced in a crack tip as a result of cyclic hydrogen pressure with a maximum of 70 MPa.

2. Diffusion model

2.1. Hydrostatic stress and trapping

Fick's laws describe ideal diffusion, i.e. when the mass transport is only due to concentration gradients. However, the stress state and the presence of defects modify hydrogen diffusion significantly. Such defects, e.g. dislocations, grain boundaries or inclusions, cause the hydrogen to be retained and are thus called hydrogen traps. Variables are distinguished depending on whether the hydrogen is in a lattice site (L subscript) or in a trapping site (subscript T) [2]. Hydrogen flux between lattice sites $\mathbf{J_L}$ is proportional to the gradient of chemical potential, which is reduced by hydrostatic stress. So the following expression is obtained:

$$\mathbf{J_L} = -D_L \nabla C_L + \frac{D_L}{RT} C_L \bar{V}_H \nabla \sigma_h \tag{1}$$

where C_L is the hydrogen concentration in lattice sites, D_L the lattice diffusivity, σ_h the hydrostatic stress, $\bar{V}_H$ the partial molar volume of hydrogen in the metal, R the universal constant of gases and T the absolute temperature. Neglecting flux between traps and distinguishing between hydrogen concentration in lattice sites C_L and in trapping sites C_T, the mass balance of total hydrogen might be expressed as:

$$\frac{dC_L}{dt} + \frac{dC_T}{dt} + \nabla \cdot \mathbf{J_L} = 0 \tag{2}$$

To find the expression of dC_T/dt a kinetic relationship between the two sites must be established. In the most generic situation the McNabb and Foster [3] formulation is required, but for simplicity here it is assumed that lattice sites and traps are in thermodynamic equilibrium, i.e. the Oriani's balance [4]:

$$\frac{\theta_T}{1-\theta_T} = \frac{\theta_L}{1-\theta_L} K_T \tag{3}$$

where $K_T = \exp(-E_b/RT)$ being E_b the binding energy of the traps; θ_L and θ_T are the lattice and trap occupancy, i.e. the hydrogen concentration divided by the concentration of sites ($\theta_L = C_L/N_L$ and $\theta_T = C_T/N_T$). N_L depends on the kind of lattice, but the number of defects N_T depends on the stress state since plastic deformation causes the creation of dislocations. The expression that relates N_T with the equivalent plastic strain ε^p is usually fitted by experimental tests. Additionally, Krom et al. [2] introduce a term derived from dC_T/dt when a dependence of N_T on plastic strain rate is taken into account. Deriving equation (3), dC_T/dC_L is inserted into the mass balance, resulting in the general diffusion equation:

$$\left(\frac{C_T(1-\theta_T)}{C_L}+1\right)\frac{\partial C_L}{\partial t}+\theta_T\frac{dN_T}{d\varepsilon^p}\frac{d\varepsilon^p}{dt}-\nabla\cdot\left(D_L\nabla C_L\right)+\nabla\cdot\left(\frac{D_L C_L\bar{V}_H}{RT}\nabla\sigma_h\right)=0 \tag{4}$$

2.2. Coupled diffusion

As it was shown in section 2.1., the stress state influences the diffusion of hydrogen. On the other hand, the presence of hydrogen modifies the elasto-plastic material response, i.e. diffusion is a coupled phenomenon. The introduced variable into the constitutive equations is the total hydrogen concentration measured as H atoms per metal atom, $c = (C_L + C_T)/N_{Me}$. Coupled diffusion modelling usually incorporates two aspects:

- Dilatation: hydrogen induces a volumetric expansion $\varepsilon^h_{vol} = c\cdot\Delta v/\Omega$, where Δv is the volume increase per hydrogen atom, and Ω is the mean atomic volume of a metal atom [5]. Hence a term corresponding to the dilatation produced by hydrogen must be added to the deformation rate tensor in the constitutive equation.
- Modified plastic flow: hydrogen affects dislocation mobility and emission from the crack tip so it modifies the plastic flow σ_{ys} [5]. This is modelled including the concentration c and a coupling parameter ξ:

$$\sigma_{ys}\left(\varepsilon^p,c\right)=\left(\xi c+1\right)\sigma_0\left(1+\frac{E}{\sigma_0}\varepsilon^p\right)^n \tag{5}$$

The expression (5) also considers work hardening as a power law where E is the Young modulus, σ_0 the initial yield stress and n the hardening coefficient. At the macroscopic scale a hydrogen-induced softening ($\xi < 0$) or hardening ($\xi > 0$) can be found.

2.3. Boundary conditions

Due to the complexity of adsorption and absorption phenomena, especially in electrochemical hydrogen charging, the boundary conditions in diffusion problems are often oversimplified. Having compressed gas stored in a vessel, dissociation of the H_2 molecule is the critical step in adsorption. For that reason, Sievert's law has been usually applied to obtain the boundary concentration in which the stress-state influence is frequently not included. However, if the chemical potential of hydrogen in solution μ_L and that of gaseous hydrogen μ_{H_2} are considered equal in the boundary, $\mu_{L,b} = \mu_{H_2}$ [6], and low occupancy is assumed θ_L<<1, the following expression results:

$$C_{L,b}=K\sqrt{f_{H_2}}\exp\left(\frac{\bar{V}_H\sigma_h}{RT}\right) \tag{6}$$

That is to say, a Sievert's law modified by the hydrostatic stress is found. $C_{L,b}$ is the implemented boundary condition in the vessel inner wall. It also should be noted that fugacity f_{H2} appears in (6) instead of the hydrogen pressure p; both can be related by the Abel-Nobel formula [7] in which b is equal to 15.84 cm^3/mol:

$$f_{H_2}=p\exp\left(\frac{bp}{RT}\right) \tag{7}$$

3. Finite Elements implementation

Simulations of the vessel have been performed in the Finite Element software ABAQUS. However, equations described in section 2 cannot be implemented by default in this code. In order to model diffusion, the mathematical analogy with heat transfer has been exploited: both flux equations and mass balance have equivalent forms. The UMATHT subroutine allows to implement the two-level diffusion model. For the purpose of accessing and storing the hydrostatic stress and the equivalent plastic strain, a USDFLD subroutine has been employed.

In addition, diffusion coupling has also been implemented by this heat transfer analogy: expansion caused by hydrogen might be regarded as a thermal expansion (UEXPAN subroutine) and the plastic flow modification is equivalent to a temperature-dependence of yield stress (UHARD subroutine).

4. Modelling

4.1. Material characterization

The AISI 4130 steel has been chosen for the simulated vessel. Its chemical composition is shown in Table 1:

Table 1. Allowable composition range (wt%) for AISI 4130 steel [8]

Component	Cr	Mo	C	Mn	Si	P	S	Other
min wt%	0.80	0.15	0.28	0.40	0.15	-	-	-
max wt%	1.10	0.25	0.33	0.60	0.35	0.035	0.040	-

Yield strength σ_{ys} and ultimate tensile strength σ_u are extracted from reference [9] where steel AISI 4130 was quenched in oil to room temperature and then tempered at 450ºC for 1.5 hours obtaining thus a tempered martensite microstructure. Young's modulus E, Poisson's coefficient ν and hardening exponent n are chosen as usual for steels.

Table 2. Mechanical parameters for AISI 4130 steel.

E (MPa)	ν	n	σ_{ys} (MPa)	σ_u (MPa)
210000	0.3	0.2	1186	1289

4.2. Diffusion parameters

For quenched and tempered 4130 steel, Arrhenius-type expressions of diffusivity D and solubility K have been found in references [8, 10]. Although permeation tests were performed at high temperatures, values are extrapolated to room temperature (298 K). Apparent diffusivity from [10] is assumed as lattice coefficient D_L because its value is very close to that found for pure iron [2], showing a little trapping influence in these permeation tests. Partial molar volume $\bar{V}_H$ of hydrogen in steel is taken as $2 \cdot 10^{-6}$ m^3/mol [2]. Number of lattice sites N_L is obtained assuming a bcc structure for martensite (for carbon content less than 0.6 mass % [11]) and tetrahedral preferred occupancy [12].

The binding energy E_b of traps is taken from [13] as the corresponding energy of a dislocation in tempered martensite. The number of trapping sites is related with equivalent plastic strain through the expression found by Kumnick and Johnson [14]:

$$\log N_T = 23.26 - 2.33 \exp(-5.5 \varepsilon^p) \tag{8}$$

Regarding the hydrogen induced dilatation, Δv and Ω are obtained assuming the usual density and atomic weight of iron. ξ parameter is equal to zero since there is no evidence of local softening or hardening in 4130 steel. All parameters are shown in Table 3:

Table 3. Diffusion parameters for AISI 4130 steel.

$D_L\left(\frac{m^2}{s}\right)$	$K\left(\frac{atH}{mol\sqrt{MPa}}\right)$	$V_H\left(\frac{m^3}{mol}\right)$	$N_L\left(\frac{sites}{m^3}\right)$	$E_b\left(\frac{kJ}{mol}\right)$	$\Delta v / \Omega$	ξ
$1.41 \cdot 10^{8}$	2.09·1021	$2 \cdot 10^{-6}$	5.09·1029	-33.9	0.2834	0

4.3. Thickness design

The two set values are: maximum internal working pressure p_w of 70 MPa and inner radius R_i of 500 mm. The ASME Boiler and Pressure Vessel Code [15] gives a value of thickness t_w assuming thin (9) or thick (10) wall:

$$t_w = \frac{p \cdot R_i}{S \cdot E - 0.6p} \tag{9}$$

$$t_w = R_i \left[\sqrt{\frac{S \cdot E + p}{S \cdot E - p}} - 1 \right] \tag{10}$$

p is the internal pressure. However, type I vessels must resist not only the working pressure; they are designed for a proof load (p = 1.5 p_w) and a burst load (p = 2.25 p_w). S is the material strength (σ_{ys} for proof load and σ_u for burst load). E is a parameter that introduces the welding efficiency in the vessel; in this case, welding influence is neglected, i.e. E = 1.

Another design option is to assume the analytical formulas for the stresses on a vessel. Hoop and radial maximal stresses ($\sigma_{\theta,\max}$, $\sigma_{r,\max}$) are obtained from the force equilibrium in a cylindrical wall with closed ends. Assuming plane strain conditions, longitudinal stress $\sigma_{z,\max}$ might also be obtained:

$$\sigma_{\theta,\max} = p \left[\frac{2R_i^2}{2R_i t_w + t_w^{\,2}} + 1 \right] \tag{11}$$

$$\sigma_{r,\max} = -p \tag{12}$$

$$\sigma_{z,\max} = \nu(\sigma_{\theta,\max} + \sigma_{r,\max}) \tag{13}$$

If $t_w << R_i$, hoop stresses might be found with the thin wall formula:

$$\sigma_{\theta,\max} = p \frac{R_i}{t_w} \tag{14}$$

Hoop stresses are often taken as the critical stresses. However, in order to refine the thickness design, the equivalent von Mises stress can be compared with the strength of the material. Considering the obtained design values shown in Table 4, a thickness of 66 mm is modelled. Being R_i / t_w = 7.57, the condition of thin wall ($R_i / t_w >$ 10) is not satisfied.

Table 4. Minimum thickness required considering different approaches.

	ASME		Analytical (hoop stress)		Analytical (von Mises stress)	
	Thin Wall	Thick Wall	Thin Wall	Thick Wall	Thin Wall	Thick wall
Proof load	46.75	46.41	44.26	46.41	42.36	44.32
Burst load	65.93	65.33	61.09	65.33	60.25	64.35

4.4. Vessel

A half of the vessel cross section is modelled in 2D considering symmetry and assuming plane strain conditions (Fig. 1. right picture). With the purpose of analyzing the stress state influence on hydrogen diffusion, a crack with a length of 5% of the thickness and 0.5 mm of root radius is introduced in the plane of symmetry.

4.5. Cyclic load

The filling time of the tank is supposed to be 5 minutes in which there is a ramp pressure from 0 to 70 MPa. Since then, a cosine periodic charge is introduced, varying the amplitude and the frequency. Four situations are simulated: (a) non-cyclic pressure of 70 MPa; (b) 70 to 50 MPa and a cycle time of 300 s; (c) 70 to 35 MPa and a cycle time of 300 s; (d) 70 to 35 MPa and a cycle time of 30 s. Load histories are depicted in left pictures in Fig. 2.

5. Results

Dotted line in Figure 1 represents C_L at 300 s, when hydrogen pressure has reached its maximum of 70 MPa. Peak concentration is located at the boundary at that moment. As hydrogen diffuses, hydrostatic stress peak drifts C_L maximum towards the bulk material, and the solid line shown in Figure 1 is achieved at steady state when chemical potential gradients have disappeared. C_L maximum at steady state is approximately 0.013 wppm. This value represent the $C_{L,\max}$ asymptote in transient analysis for long times. Hydrogen concentration in trapping sites C_T is always two or three orders of magnitude less than C_L since there is no a significant level of plastic strain and dislocations have a low binding energy. As a consequence, total hydrogen concentration might be identified with C_L.

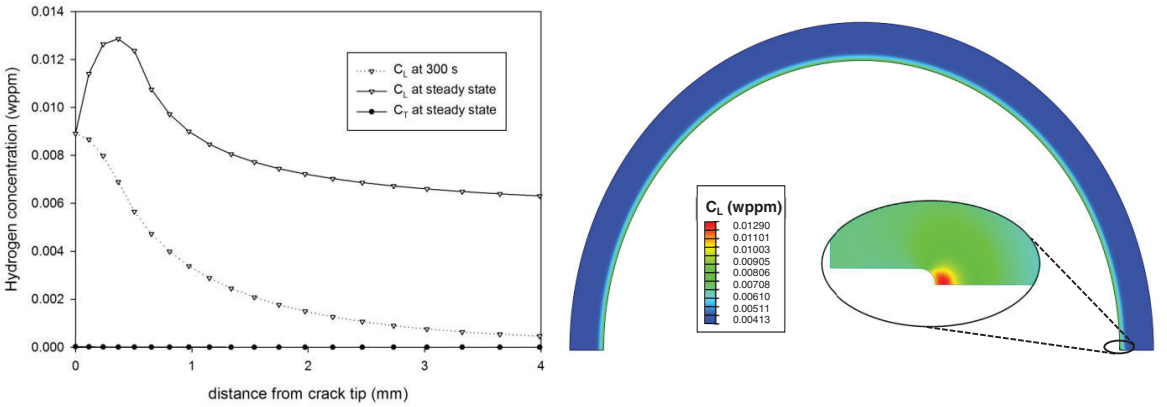

Fig. 1. Hydrogen distribution C_L and C_T in the symmetry axis (left); hydrogen distribution near the crack tip at steady state (right).

When pressure is maintained constant after the initial ramp (situation (a) in Figure 2), maximum hydrogen concentration is reached at the boundary, i.e. $C_{L,b} = C_{L,\max}$. Since approximately 1400 s, $C_{L,\max}$ increases because a peak is appearing at a certain distance from crack tip.

As load amplitude is increased, i.e. $R = p_{min}/p_{max}$ is reduced, $C_{L,\max}$ rises slower because of the boundary condition influence. At 3300 s, $C_{L,\max}$ reaches 0.0119 wppm for R = 1, whereas for R = 0.714 only reaches 0.0110 wppm and for R = 0.5 only 0.00998 wppm (respectively: (a), (b) and (c) situations in Figure 2). The range of $C_{L,b}$ is associated also with this amplitude.

$C_{L,\max}$ peaks are slightly delayed respect those of $C_{L,b}$; this represents the times it takes hydrogen to diffuse from the crack tip to the region of high hydrostatic stress. Nonetheless, when frequency is increased (t_{cycle} = 30 s in (d) in Figure 2), hydrogen does not have time to diffuse in such a short cycle time and thus the $C_{L,\max}$ peak coincides with that of $C_{L,b}$ at the moment in which the pressure is 70 MPa. Therefore, C_L peaks of 0.00938 wppm never rise.

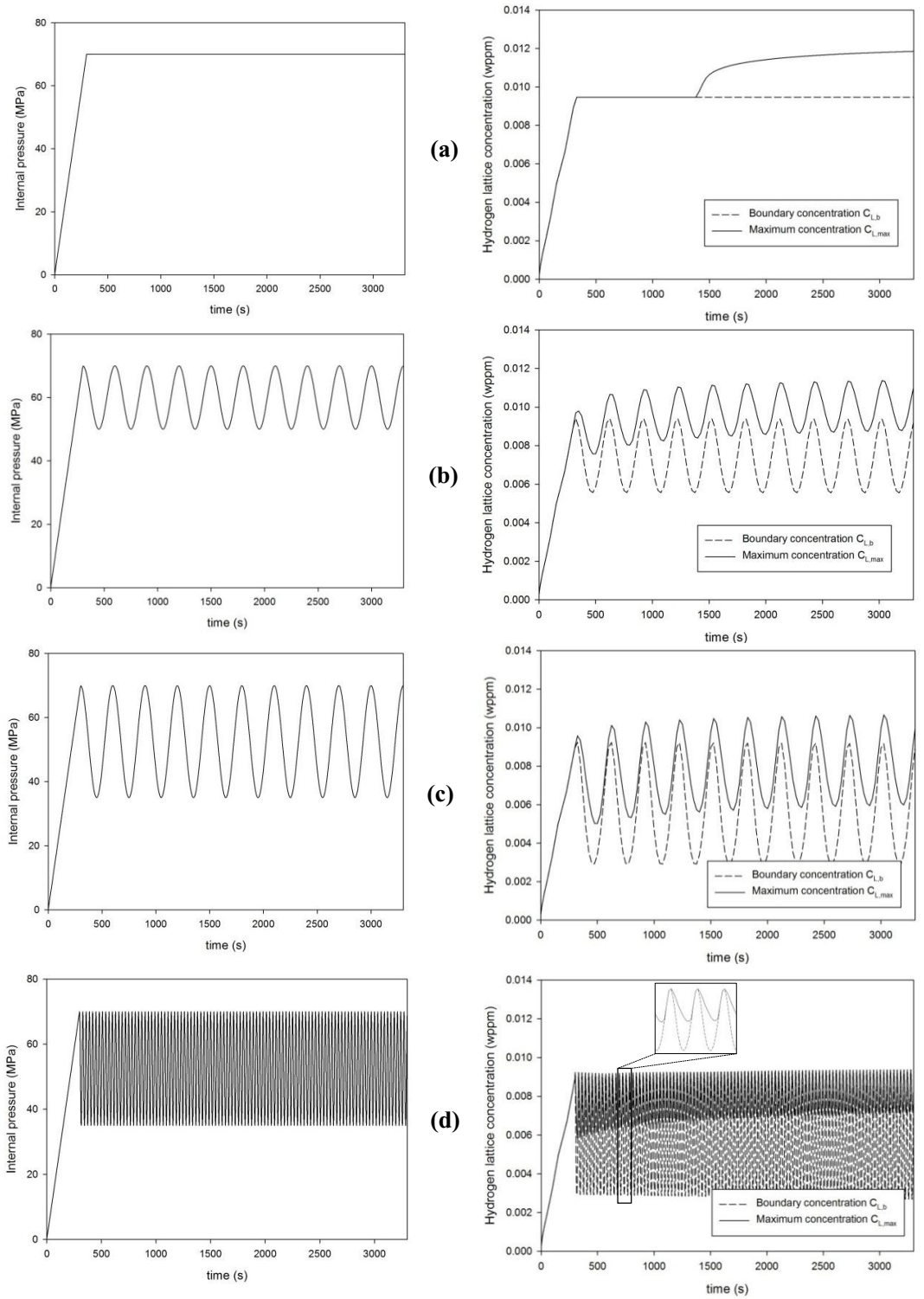

Fig. 2. Left pictures: load history; right pictures: C_L at crack tip boundary (dashed line) and maximum C_L (solid line). (a) R=1.0; (b) R = 0.714, t_{cycle} = 300 s; (c) R = 0.5, t_{cycle} = 300 s; (d) R = 0.5, t_{cycle} = 30 s.

6. Conclusions

During their lifetime, pressure vessels containing hydrogen experience cyclic loads. When internal pressure p is a cyclic load, it influences the hydrogen distribution in two senses: through the fugacity and through the stress state produced in the vessel. In order to analyse the crack initiation and propagation it is essential to know how hydrogen is redistributed when stress state, and thus boundary condition, is not constant.

When hydrogen transport evolves, a concentration peak appears due to the hydrostatic stress distribution. In the simulated tank, the maximum concentration at steady state is equal to 0.013 wppm. This value is a consequence of the low solubility of hydrogen in steel. However, embrittlement might occur in high strength steels with small concentrations.

In this paper, trapping influence is implemented in diffusion equations. However, hydrogen is hardly retained in traps because of the low binding energy found for dislocations in tempered martensite. Other kind of traps should be better characterized by different tests in AISI 4130 steel since, in many cases, C_T could be not negligible.

In high pressure environments, load amplitude is a crucial magnitude in hydrogen diffusion: the smaller is the amplitude, the faster the maximum steady state concentration is achieved for a fixed maximum pressure. Frequency is also an important parameter: as shown in some fatigue tests [16], steels are less embrittled at high frequencies because there is not enough time for hydrogen to diffuse towards the Fracture Process Zone. Results in this paper also indicate that the higher the frequency, the lower the maximum concentration reached.

Acknowledgements

The authors are grateful for the funding received from project MCI Ref: MAT2014-58738-C3-2-R.

References

[1] J. Zheng, X. Liu, P. Xu, P. Liu, Y. Zhao, J. Yang. Development of high pressure gaseous hydrogen storage technologies, International Journal of Hydrogen Energy 37 (2012) 1048-1057.

[2] A.H.M. Krom, R.W.J. Koers, A. Bakker. Hydrogen transport near a blunting crack tip, Journal of the Mechanics and Physics of Solids 47 (1999) 971-992.

[3] A. McNabb, P.K. Foster. A new analysis of the diffusion of hydrogen in iron and ferritic steels, Transactions of the Metallurgical Society of AIME 227 (1963) 618-627.

[4] R.A. Oriani. The diffusion and trapping of hydrogen in steel, Acta Metallurgica 18 (1970) 147-157.

[5] Y. Liang, P. Sofronis, N. Aravas. On the effect of hydrogen on plastic instabilities in metals, Acta Materialia 51 (2003) 2717-2730.

[6] C.V. Di Leo, L. Anand. Hydrogen in metals: A coupled theory for species diffusion and large elastic–plastic deformations, International Journal of Plasticity 43 (2013) 42-69.

[7] C.S. Marchi, B.P. Somerday, S.L. Robinson. Permeability, solubility and diffusivity of hydrogen isotopes in stainless steels at high gas pressures, International Journal of Hydrogen Energy 32 (2007) 100-116.

[8] C. San Marchi, B.P. Somerday. Technical reference on hydrogen compatibility of materials. SAND2012-7321 (2012)

[9] P.S. Song, Y.L. Shieh. Fracture lifetime of hydrogen-charged AISI 4130 alloy steel under intermittent sustained overloads, Engineering Fracture Mechanics 71 (2004) 1577-1584.

[10] H.G. Nelson, D. Williams. Quantitative observations of hydrogen-induced, slow crack growth in a low alloy steel, NASA-TM-X-62253 (1973).

[11] O.D. Sherby, J. Wadsworth, D.R. Lesuer, C.K. Syn. Revisiting the structure of martensite in iron-carbon steels, Materials transactions 49 (2008) 2016-2027.

[12] A.H. Krom, A. Bakker. Hydrogen trapping models in steel, Metallurgical and materials transactions B 31 (2000) 1475-1482.

[13] F.-G. Wei, K. Tsuzaki. Response of hydrogen trapping capability to microstructural change in tempered Fe–0.2C martensite, Scripta Materialia 52 (2005) 467-472.

[14] A. Kumnick, H. Johnson. Deep trapping states for hydrogen in deformed iron, Acta Metallurgica 28 (1980) 33-39.

[15] Boiler and Pressure Vessel Code. American Society of Mechanical Engineers, Section VII, (2015).

[16] S. Matsuoka, H. Tanaka, N. Homma, Y. Murakami. Influence of hydrogen and frequency on fatigue crack growth behavior of Cr-Mo steel, International Journal of Fracture 168 (2011) 101-112.